

# Performance optimization of reconfigurable optical add-drop multiplexers employing opto-VLSI processors

Mingya Shen\*, Feng Xiao, and Kamal Alameh  
Centre of Excellence for MicroPhotonic Systems, Edith Cowan University, Joondalup,  
WA, 6027, Australia

## ABSTRACT

In this paper, we propose and experimentally demonstrate the principle of a novel reconfigurable optical add-drop multiplexer (ROADM) structure employing an Opto-VLSI processor. The ROADM structure integrates two arrayed waveguide gratings for wavelength division multiplexing and demultiplexing, a 4-f imaging system comprising a fiber array, an imaging lens array and a reflective Opto-VLSI processor. The Opto-VLSI processor is driven by phase holograms to switch the various wavelength channels between the fiber ports to achieve “through” or “drop” operations. Phase hologram optimization is investigated, for maximising the number of wavelength channels while keeping adequate insertion loss and crosstalk levels. Experimental results are shown, which demonstrate the principle of the ROADM with crosstalk of less than -30dB and insertion loss of less than 6dB for the drop and through operation modes.

**Keywords:** Wavelength division multiplexing, optical switching, liquid crystal on silicon

## 1. INTRODUCTION

In dynamic wavelength-division multiplexing (WDM) optical communication networks, a Reconfigurable Optical Add-Drop Multiplexer (ROADM) enables individual or multiple wavelength channels to be added and/or dropped from a transport fiber without the need for optical-to-electrical-to-optical conversion. The use of ROADMs in optical networks provides dynamic allocation of the available network bandwidth to individual users without affecting the traffic. It also enables equalization of the power levels of the different wavelength channels processed through the ROADM [1], [2]. ROADM structures based on micro-electro-mechanical systems (MEMS) have been reported [3], which use micro-mirrors for steering optical beams to be coupled into different destinations. Planar lightwave circuits (PLCs) have also been deployed for realizing ROADM structures [4]. Opto-VLSI processors have recently been used for achieving add/drop multiplexing [5], [6], where add/drop multiplexing of a large number of wavelength channels is achieved through computer-generated phase holograms that steer optical beams between fiber ports.

In this paper, we investigate the performance optimization of a new ROADM structure employing commercially-available array of parallel optical fiber pairs in conjunction with an Opto-VLSI processor and an array of 4-f imaging microlenses that are offset in relation to the axis of symmetry of the parallel fiber pairs. By partitioning the Opto-VLSI processor into pixel blocks and driving each pixel block with optimized “drop” or “thru” steering phase hologram, optical switching between each paired optical fiber can be realized, leading to optical add/drop multiplexing. The performance of the add-drop multiplexing of the ROADM structure is optimised through hologram parameter optimization, which results in moderate insertion loss and crosstalk, especially when the ROADM is constructed using off-the-shelf optical components.

## 2. STRUCTURE AND PRINCIPLE OF THE ROADM

### 2.1 The Opto-VLSI Processor

An Opto-VLSI processor consists of liquid crystal (LC) cells and Very-Large-Scale-Integrated (VLSI) circuits that drive an array of LC cells [7]. It can generate multi-phase holographic blazed gratings capable of steering or shaping optical

\* m.shen@ecu.edu.au; phone 61 8 63042572; fax 61 8 63045302

beams, as illustrated in Fig. 1. Each pixel of the Opto-VLSI processor is independently driven by a discrete voltage applied between the aluminum mirror electrode across the LC cells and a transparent Indium-Tin Oxide (ITO) layer as the second electrode. A quarter-wave-plate (QWP) layer between the LC and the aluminum mirror is usually used to accomplish polarization-insensitive operation [8]. An Opto-VLSI processor is electronically controlled, software configurable and has the capability of controlling multiple optical beams simultaneously with no mechanical moving parts.

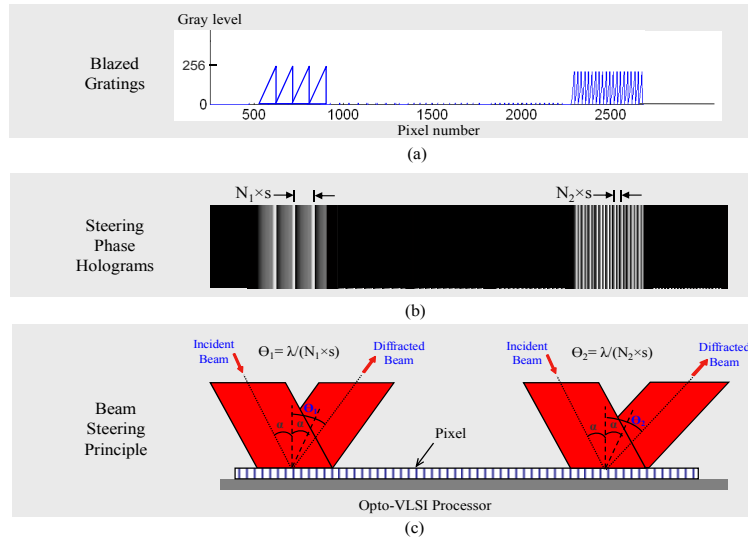


Fig. 1. (a) Gray level versus pixel number of different blazed gratings; (b) Corresponding steering phase holograms; (c) Principle of beam steering using an Opto-VLSI processor. The steering angle is inversely proportional to the blazed grating period.

## 2.2 Opto-VLSI-based ROADM Structure

Fig. 2 shows the proposed Opto-VLSI-based reconfigurable ROADM structure employing an off-axis 4-f imaging system for add/drop multiplexing. The input WDM signals are routed, through a circulator, to an N-channel arrayed

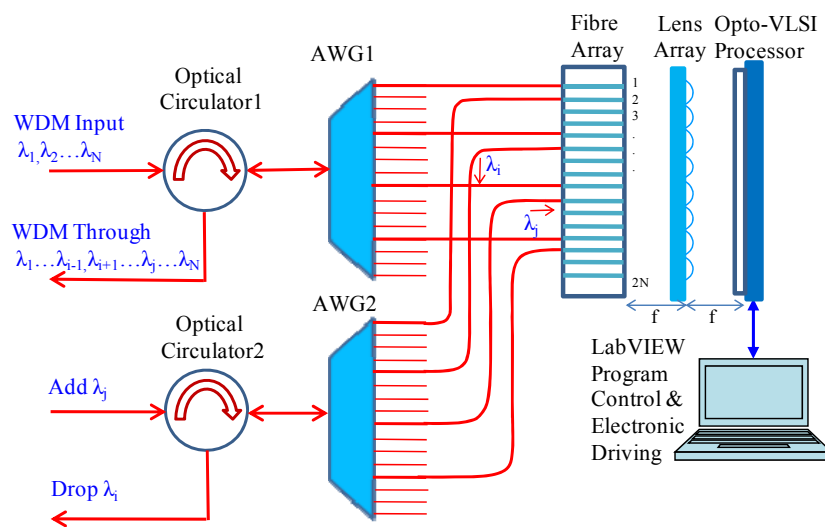


Fig. 2. The Opto-VLSI based ROADM structure using two AWGs, arrayed fiber pairs and a lens array realizing any reconfigurable add-drop and through operations of wavelength signals.

waveguide grating (AWG1) demultiplexer whose output fiber ports correspond to wavelength channels ( $\lambda_1$  to  $\lambda_N$ ). The AWG1 ports are connected to the odd-numbered ports of a fiber array, which consists of  $N$  fiber pairs. Each fiber pair comprises an upper fiber (connected to AWG1) and a lower fiber (connected to AWG2). A lens array is placed at a distance equals to the focal length  $f$  of the lens elements from the fiber array. Each lens collimates the divergent beam from its corresponding upper optical fiber. The spacing between the upper fiber and the optical axis of the associated lens is approximately a quarter of the fiber array spacing. The collimated optical beams (wavelength channels) are mapped on the active window of the Opto-VLSI processor that is placed at a distance  $f$  from the lens array.

### 2.3 4-f Imaging System

Fig. 3 illustrates the principle of add/drop multiplexing for wavelength channels in the ROADM structure shown in Fig. 2. When a blank phase hologram drives a pixel block associated to a fiber pair, the optical beam diverging from an upper optical fiber is collimated by the 4- $f$  imaging lens associated to the fiber pair, reflected back by the Opto-VLSI processor ( $0^{\text{th}}$ -order diffraction), and then focused by the same lens onto a spot between the upper and lower optical fibers so that negligible optical power is coupled into both upper and lower fibers appearing as crosstalk, which is illustrated in Fig. 3(a). By driving the Opto-VLSI processor with optimised steering holograms, a collimated beam can be steered and coupled to either the lower fiber ( $+1^{\text{st}}$ -order diffraction for drop operation) or back to the upper fiber ( $-1^{\text{st}}$ -order diffraction for thru operation) as illustrated in Fig. 3(b) and Fig. 3(c), respectively. Dropped channels are multiplexed via the second arrayed waveguide grating (AWG2) and routed through a circulator to the drop port. The added wavelengths are launched at the add-port propagate along the same paths of the AWG2 input but in a different output path of the AWG2 connected to the lower paired fiber. They are steered by the Opto-VLSI processor, coupled to the upper fibers and multiplexed via AWG1 to reach the thru port.

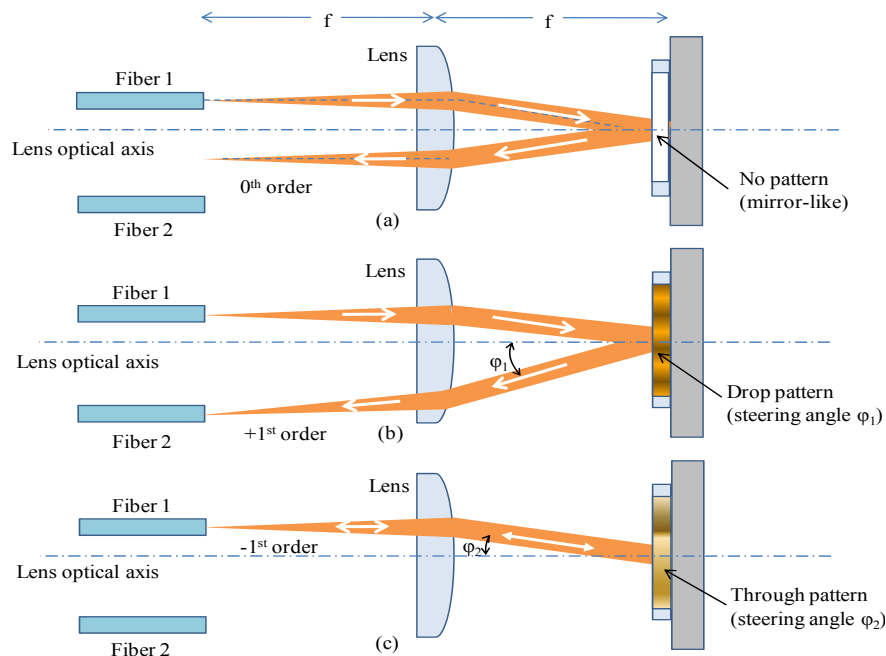


Fig. 3. Illustration of the principle of drop and thru operations. The upper and lower fibers are offset from the optical axis of their associated imaging lens for achieving optical switching between the fibers with minimum crosstalk. (a) Without a hologram, the collimated optical beam reflects back and focuses on a spot between the two fibers; (b) With a drop hologram on, a  $+1^{\text{st}}$  order diffracted beam is focused on and coupled into the fiber 2; (c) With a thru hologram on, a  $-1^{\text{st}}$  order diffracted beam is focused on and coupled back into the fiber 1.

### 3. EXPERIMENT RESULTS

Fig. 4 shows the experimental setup used to demonstrate the add-drop and thru performance and the feasibility of the proposed ROADM structure. A 1-D 256-gray-level 4,096-pixel Opto-VLSI processor was used, where each pixel has an area of  $6\text{mm} \times 1\mu\text{m}$  with a dead space between adjacent pixels of  $0.8\mu\text{m}$ . A 16-port fiber array of spacing  $250\mu\text{m}$  was aligned to a 4-element lens array of focal length  $2.5\text{mm}$  and spacing  $1\text{mm}$ . The Opto-VLSI processor was also aligned to and placed at around  $2.5\text{mm}$  from the lens array, thus forming a 4-f imaging system. To demonstrate the principle of drop and thru operations for the ROADM structure, four phase holograms were optimized to steer two wavelength channels at  $\lambda_1=1547.5\text{nm}$  and  $\lambda_2=1530.3\text{nm}$  generated using two tunable laser sources and launched into port 1 and port 5 of the fiber array for simulating “input” and “add” signals, respectively. The optical beam diverging from fiber port 1 was collimated at around  $0.5\text{mm}$  diameter and steered by the synthesized phase holograms either to fiber port 1 for thru operation or to fiber port 2 for drop operation. Similarly, the other wavelength channel  $\lambda_2=1530.3\text{nm}$  was simultaneously launched into fiber port 5, and through different optimized phase holograms. It was then either dropped to fiber port 6 or sent back to fiber port 5 for thru operation. Note that both input collimated optical beams (at  $\lambda_1$  and  $\lambda_2$ ) hit the Opto-VLSI processor at an angle of incidence of approximately  $1.5^\circ$ . In the experimental setup shown in Fig. 4, the two optical circulators were used to route the thru signals, and the two 3-dB couplers were used to combine the two wavelength channels ( $\lambda_1$  and  $\lambda_2$ ) so they can be monitored simultaneously by a single optical spectrum analyzer (OSA).

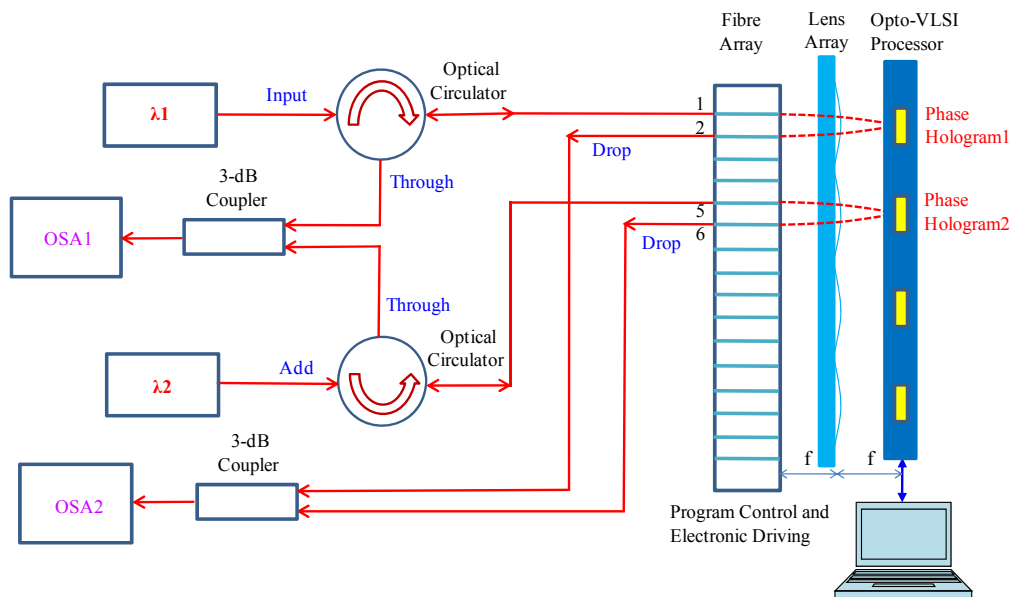


Fig. 4. Experimental setup demonstrating the principle of add/drop and thru operations for the Opto-VLSI-based ROADM structure. The 4-f imaging system is composed of a fiber array, a lens array and an Opto-VLSI processor with phase holograms loaded.

To investigate the dependence of drop/thru loss and crosstalk on hologram size (i.e. number of pixels), we optimized the parameters (the ramp parameters and the grating period) of the steering hologram with the center of the incident Gaussian beam projected onto the center of the hologram and the number of pixels driven by the blazed grating varied. For each hologram size, the signals coupled into the drop and thru ports were monitored by two optical spectrum analyzers. Fig. 5 shows the measured dropped signal power at fiber 2 and crosstalk at fiber 1 versus the hologram size (in pixels). It is noted that for a hologram size of 250 pixels, the crosstalk level is less than 30dB where the crosstalk is defined as the ratio of the thru (or dropped) power at  $\lambda$  to the power at  $\lambda$  received at the drop port (or thru port), and that the drop/thru insertion loss is not significantly improved if the hologram size is increases beyond 250 pixels.

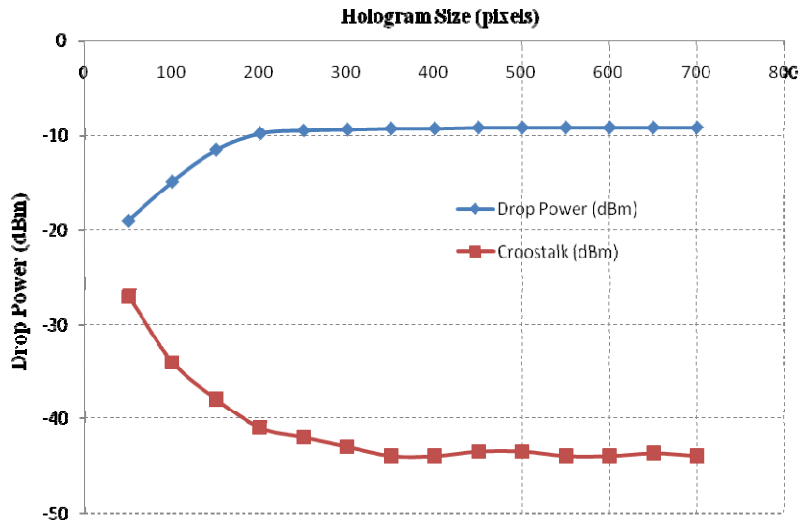


Fig. 5. Experimental measurement results for the power levels of the drop signals (upper trace) at fiber 2 and crosstalk (bottom trace) appearing at fiber 1.

Fig. 6 shows the optimized phase holograms used for drop and thru operations. Note that a LabVIEW program was especially written to control the Opto-VLSI processor so that “drop” and “thru” operations were carried out through software only.

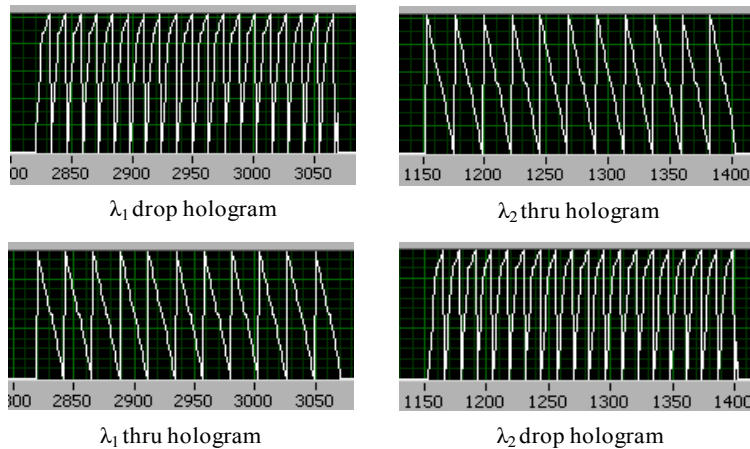
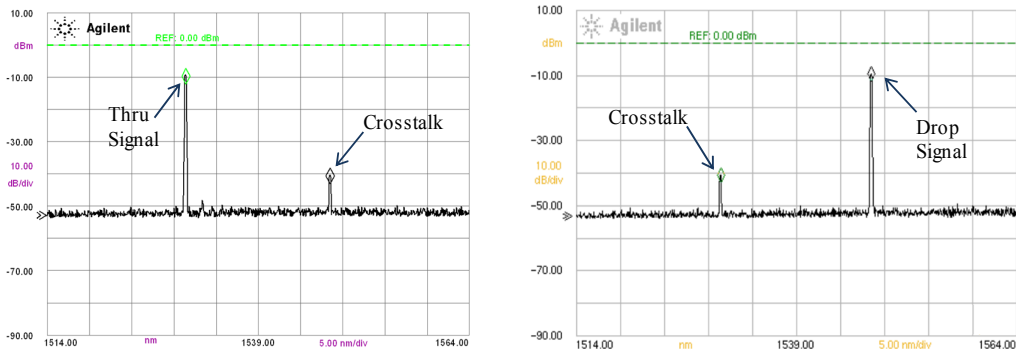


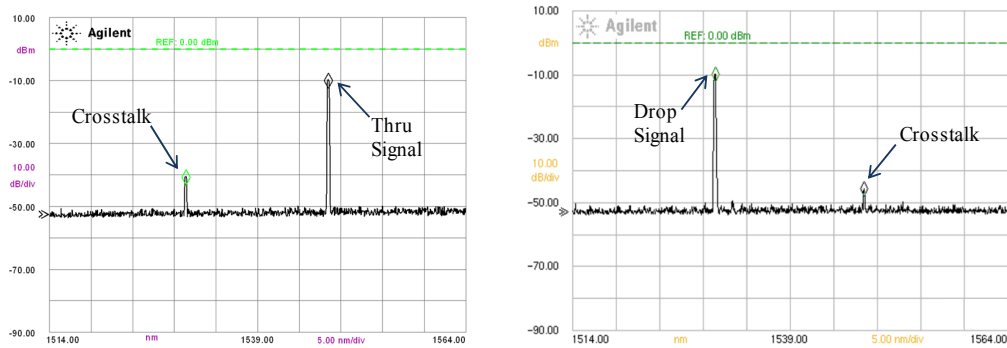
Fig. 6. Optimized “drop” and “thru” phase holograms for channels  $\lambda_1$  and  $\lambda_2$ . The horizontal axis is in units of pixels and the vertical axis is gray level from 0 to 256.

Fig. 7(a) shows the optical spectra measured by the two OSAs when  $\lambda_1$  (1530.5nm) is dropped and  $\lambda_2$  (1547.5nm) is passed thru, and Fig. 7(b) shows the optical spectra measured by the two OSAs when  $\lambda_1$  is passed thru and  $\lambda_2$  is dropped. Apart from the optimized hologram size of 250 pixels, other parameters including the amplitude and shape of the phase ramps and the periods of each hologram were optimized to obtain the maximum drop/thru signal power while keeping minimum crosstalk level detected. It can be seen from Fig. 7 that a crosstalk level less than -30.5dB is maintained for the different operations of the ROADM. The input optical power levels for both signals  $\lambda_1$  and  $\lambda_2$  were +1dBm, the 3-dB coupler at the thru and the drop ports introduced around 3.3dB loss, and the circulator loss was 1.6dB. Therefore, with a measured output signal power of around -9.8dBm as shown in Fig. 7 the total insertion loss of the experimental ROADM

structure was around 6dB. This loss was mainly contributed by the fiber-to-fiber beam coupling loss, the Opto-VLSI processor loss including a polarization dependent loss of 0.6dB.



(a).  $\lambda_1$  drop and  $\lambda_2$  thru signals displayed on OSA1(right side) and OSA2(left side), respectively.



(b).  $\lambda_1$  thru and  $\lambda_2$  drop signals displayed on OSA1(right side) and OSA2(left side), respectively.

Fig. 7. Experimental results showing the drop and thru operations for  $\lambda_1$  and  $\lambda_2$  channels. Measured optical spectra on OSA1 and OSA2, (a) when  $\lambda_1$  is dropped and  $\lambda_2$  is passed thru, (b) when  $\lambda_1$  is passed thru and  $\lambda_2$  is dropped.

Note that, the 1-dimensional (1-D) ROADM structure could easily be extended to a 2-dimensional (2-D) structure by using a 2-D large-area Opto-VLSI processor [9] in conjunction with a 2-D fiber array and a 2-D microlens array. This dramatically increases the number of WDM channels that can be added and dropped, and significantly reduces the per-channel cost of manufacturing the proposed ROADM structure.

#### 4. CONCLUSION

A reconfigurable optical add-drop multiplexer structure based on the use of Opto-VLSI in conjunction with arrayed waveguide gratings and an off-axis 4-f imaging system has been optimized and demonstrated for the performance experimentally. The use of a 4-f imaging system has enabled the switching of various wavelength channels between fiber pairs thus realizing add/drop multiplexing with low insertion loss and crosstalk. Measured results have demonstrated that 250 pixels is an optimal hologram size for adequate loss and crosstalk levels of less than 6dB and -30dB, respectively, for drop and thru operations.

## REFERENCES

- [1] Peter J. Winzer, et al, "100-Gb/s DQPSK transmission: from laboratory experiments to field trials," *J. Lightwave Technology*, Vol. 26, No. 20, 3388-3402, (2008).
- [2] Ronald S. Bernhey, Muzaffer Kanaan, "ROADM Deployment, Challenges, and Applications," *Proc. OFC/NFOEC*, 1-3, (2007).
- [3] Michelle Muha, Brian Chiang, and Robert Schleicher, "MEMS Based Channelized ROADM Platform," *Proc. OFC/NFOEC*, 1-3, (2008).
- [4] Eldada, L.; Fujita, J.; Radojevic, A.; Izuhara, T.; Gerhardt, R.; Jiandong Shi; Pant, D.; Wang, F.; Malek, A., "40-channel ultra-low-power compact PLC-based ROADM subsystem," in *Proc. OFC/NFOEC, NThC4*, (2008).
- [5] B. Fracasso, J. L. de Bougrenet de la Tocnaye, M. Razzak, and C. Uche, "Design and performance of a versatile holographic liquid-crystal wavelength-selective optical switch," *J. Lightwave Technology*, Vol. 21, No. 10, 2405-2411, (2003).
- [6] G. Baxter, S. Frisken, D. Abakoumov, H. Zhu, I. Clark, A. Bartos and S. Poole, "Highly programmable wavelength selective switch based on liquid crystal on silicon switching elements," in *Proc. OFC/NFOEC, OTuF2*, (2006).
- [7] Jay Stockley and Steve Serati, "Advances in liquid crystal beam steering," Boulder Nonlinear Systems, [www.bnonliner.com](http://www.bnonliner.com), (2004).
- [8] Kristina M. Johnson, Douglas J. McKnight, and Ian Underwood, "Smart Spatial Light Modulators Using Liquid Crystals On Silicon," *IEEE J. Quantum Electronics*, Vol. 29, No. 2, 699-714, (1993).
- [9] Michaël A. F. Roelens, Steven Frisken, Jeremy A. Bolger, Dmitri Abakoumov, Glenn Baxter, Simon Poole, and Benjamin J. Eggleton, "Dispersion Trimming in a Reconfigurable Wavelength Selective Switch," *Journal of Lightwave Technology*, Vol. 26, No. 1, 73-78, (2008).